Polymer Journal, Vol. 13, No. 3, pp 273–281 (1981)

Phase Separation and Viscoelastic Behavior of Semicompatible Polymer Blends: Poly(vinylidene fluoride)/ Poly(methyl methacrylate) System

Yasushi HIRATA† and Tadao KOTAKA*

Department of Macromolecular Science, Osaka University, Toyonaka, Osaka 560, Japan

(Received September 3, 1980)

ABSTRACT: Thermal and dynamic mechanical analyses of variously processed blends of poly(vinylidene fluoride) (PVF_2) and poly(methyl methacrylate) (PMMA) were carried out to elucidate the effects of lower-critical-solution-temperature (LCST) behavior reported earlier by Paul on the morphologies and properties of this system. The two components are miscible in the blends with PVF_2 content $\phi_w < 0.6$. Such blends exhibit single glass transition at T_g's, which follow the Gordon–Taylor scheme. On the other hand, the blends with $\phi_w > 0.6$, prepared by melt-mixing and annealing at 200°C for a sufficiently long period of time, exhibit two T_g's and two T_m's, implying a four-phase morphology. In such blends an LCST-type phase separation has taken place at a temperature as low as 200°C to give an amorphous mixture with $\phi_w \cong 0.6$ and a nearly pure PVF_2 melt. Quenching of such melts leads to a four-phase morphology composed of a mixed amorphous phase with $T_g \cong 55$°C, an imperfect crystalline phase grown out from the mixture and hence having a low T_m, and a nearly pure semicrystalline PVF_2 domains similar to form II crystals with $T_g \cong -40$°C and a higher T_m.

KEY WORDS Amorphous Polymer Crystalline Polymer Blends / Semicompatible Polymer Blend / Poly(vinylidene fluoride) / Poly(methyl methacrylate) / Phase Separation / Differential Scanning Calorimetry / Viscoelastic Properties / Melt-Mixed Blend / Solution-Mixed Blend /

Polymer blends of poly(vinylidene fluoride) (PVF_2) and poly(methyl methacrylate) (PMMA) have been the subject of several recent studies.[1–9] The general conclusion is that these components are miscible in the amorphous state, *i.e.*, above the melting point of PVF_2 ($T_m \cong 170$°C). Below T_m the PVF_2 crystallizes from the melt, especially with high PVF_2 content, ϕ_w, if the blend is kept above its glass-transition temperature, T_g. The blend forms a two-phase system consisting of a PVF_2 crystalline phase and a mixed amorphous phase. In short, this system is a typical example of a semicompatible polymer blend composed of a semicrystalline polymer and an amorphous polymer, in which phase separation occurs only by crystallization of the former. However, Paul *et al.*[6] pointed out that this system exhibits lower-critical-solution-temperature (LCST) behavior with cloud points, T_p, in a temperature range of about 330°C for blends with high ϕ_w. The T_p are far above the ceiling temperature for PMMA ($T_d \cong 220$°C). Such an LCST behavior, if it really exists, might bring about additional complications to the phase-separation behavior and physical properties of PVF_2/PMMA blends. If fact, there are certain discrepancies between reported T_g *versus* composition data for melt-mixed blends[2,5] and for solvent-cast blends[3] of this system. Thus, we have attempted to resolve these problems by comparing the thermal and dynamic mechanical behavior of melt blends with that of solvent-cast blends of this system. The results obtained are reported in this paper.

† Present address: *Research and Development Department, Bridgestone Tire Co., 2800-1 Ogawahigashimachi, Kodaira 187, Japan.*

* To whom correspondence should be addressed.

EXPERIMENTAL

Materials

The PVF_2 used in this study was a powder-form sample (KF Polymer 1100) purchased from Kureha Kasei Co., while three PMMA samples were prepared at our laboratory by a radical-polymerization method with azobis-isobutylonitrile as the initiator. For purification of the samples, the PVF_2 was dissolved in hot acetone and precipitated in excess water, while the PMMA samples were dissolved in benzene and precipitated in excess methanol. For each sample the procedure was repeated twice. Molecular weights and the distributions of the PMMA samples were determined on a gel-permeation chromatograph (GPC: Toyo Soda Mfg. Co., Model HCL-801A) with tetrahydrofuran (THF) as carrier. Characterization data[10] are given in Table I.

Preparation of Blends

(a) Melt-Mixed Blends. The PVF_2 and PMMA samples were mixed and kneaded in a mortar with a small amount of water to form a paste. This paste was dried, hot-pressed into films at 200°C for 20 minutes, and then quenched in liquid N_2. The film was then cut into pieces, which were remelted and hot pressed at 200°C for 20 minutes, and quenched in liquid N_2. To obtain well-mixed, homogeneous specimens for the later measurements, we repeated the melting-quenching process at least 15 times, since a preliminary test on a PVF_2/PMMA III (50/50 by weight) blend indicated that the degree of crystallinity, the T_g, the T_m, and other thermal and mechanical properties of the blend appoached to constant values only after repeating this procedure at least from 10 to 20 times. These specimens were coded as melt-quenched (MQ) blends. Some of the MQ blends were further annealed at a desired temperature, t°C, controlled within ± 1°C for 16 hours. They were coded as melt-annealed [MA(t°C)] blends.

(b) Solution-Mixed Blends. Films were prepared by casting from 3% *N,N*-diemthylformamide (DMF) solutions according to the method described by Nishi and Wang.[3] The as-cast films were coded as solvent-cast (S) blends. Again, some of these films were heat-treated at 200°C in a hot-press for a certain period of time (t min), and then quenched in liquid N_2. The films were coded as solvent-cast-melt-quenched [SM(t min)Q] blends.

Methods

The dynamic mechanical measurements were made with a Rheovibron Model DDV-II dynamic viscoelastometer (Toyo-Baldwin Co., Tokyo) at a heating rate of about 1°C min^{-1}. The frequency was 110 Hz and the temperature range was from -120°C to 170°C. For the calorimetric study a Rigaku Denki (Tokyo) Model YDSM differential scanning calorimeter was used at a heating rate of 10°C min^{-1} in the range from -70°C to 220°C.

RESULTS

Behavior of Melt-Mixed Blends

The data given in this and in the following sections were obtained on PVF_2–PMMA II blends, unless otherwise specified.

(a) Thermal Behavior. Figure 1 shows several

Table I. Homopolymer characterization data

Sample	$M_n \times 10^{-4}$	$M_w \times 10^{-4}$	M_w/M_n	Source[a]
PVF_2	7[b]	...	...	Kureha KF polymer 1100
PMMA I	5.9	10	1.7	Solution polymerization in toluene at 58°C for 4.5 h. [I]=7, [M]=80
PMMA II	12	30	2.5	Bulk polymerization at 90°C for 1 h. [I]=0.5
PMMA III	200	340	1.7	Bulk polymerization at 58°C for 1 h. [I]=2.5×10^{-3}

[a] [I], AIBN mol%; [M], MMA mol%.
[b] From Manufacturer's catalogue. Data for PMMAs were obtained by GPC with THF carrier.

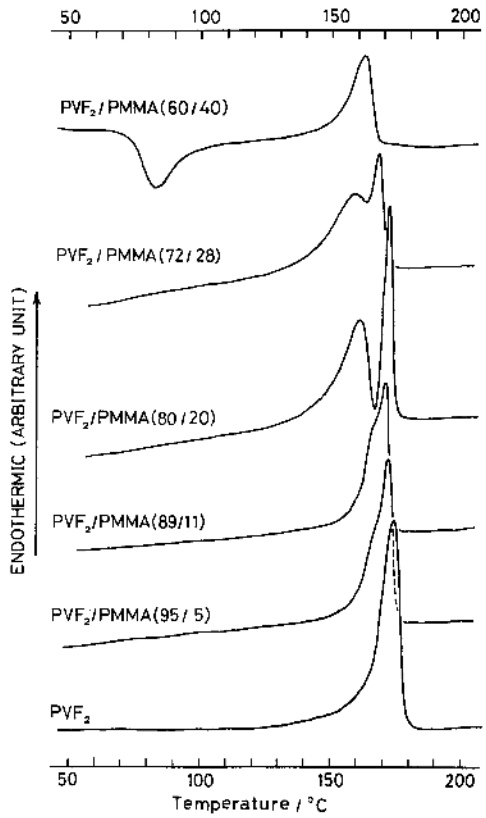

Figure 1. DSC thermograms for crystallization and melting of PVF_2 in PVF_2/PMMA II (MQ) blends with high content $\phi_w > 0.6$, obtained at a heating rate of 10°C min^{-1}.

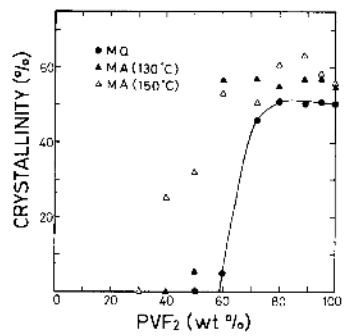

Figure 2. Dependence of degree of crystallinity, X_c, of PVF_2 on weight percent of PVF_2, ϕ_w, in melt-mixed blend as determined by DSC.

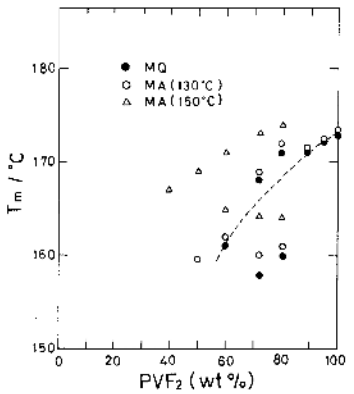

Figure 3. Dependence of melting point, T_m, of PVF_2 crystals on weight percent of PVF_2, ϕ_w, in melt-mixed blends as determined by DSC.

examples of the differential scanning calorimetry (DSC) thermograms for crystallization and melting of PVF_2 in PVF_2/PMMA II (MQ) blends with high PVF_2 content, ϕ_w (by weight). For those with $\phi_w < 0.6$ neither crystallization nor melting peaks were observed, implying that the two components are in the amorphous state and presumably mixed with each other. However, for MQ (60/40) blend, both exothermic crystallization and endothermic melting peaks were observed, indicating that crystallization of PVF_2 took place during the DSC measurement. Interestingly, for the MQ (72/28) and (80/20) blends, we observe no crystallization peaks but two melting peaks. Presumably, in the MQ (72/28) and (80/20) blends, crystallization of PVF_2 proceeded rapidly almost to the completion during the quenching process. The two peaks merged into an endothermic peak with a small shoulder and finally into a single peak of pure PVF_2 as ϕ_w underwent a further increase. Apparently these two peaks imply the presence of two different crystals.

Annealing of MQ blends at an adequate temperature, T_c, below the T_m resulted in the formation of PVF_2 crystals. For MA blends with ϕ_w as low as 0.4 crystallization and melting peaks became observable, and also for MA blends with $\phi_w > 0.4$ the area under the melting peaks grew larger than that of the corresponding MQ blends. Figures 2 and 3 show, respectively, the ϕ_w dependence of the degree of crystallinity, X_c, and that of the peak temperatures, T_m, for melting of PVF_2 crystals in the MQ and MA (t°C) blends. The values of X_c are ratios of the specific enthalpies of fusion of PVF_2 in the blend and in the homopolymer ($\cong 18$ cal g^{-1}).[11] For

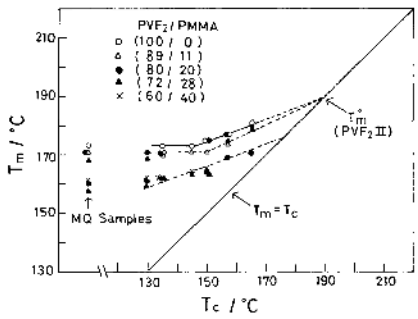

Figure 4. Plots of the melting point, T_m, of PVF_2 crystals in the melt-mixed blends *versus* the crystallization (annealing) temperature, T_c.

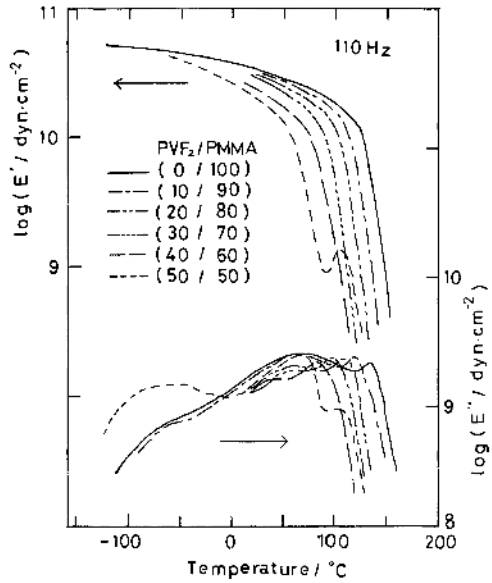

Figure 5. Dependence of dynamic storage, E', and loss, E'', moduli observed at the frequency of 110 Hz for amorphous MQ blends with the PVF_2 content, $\phi_w \leqq 0.5$.

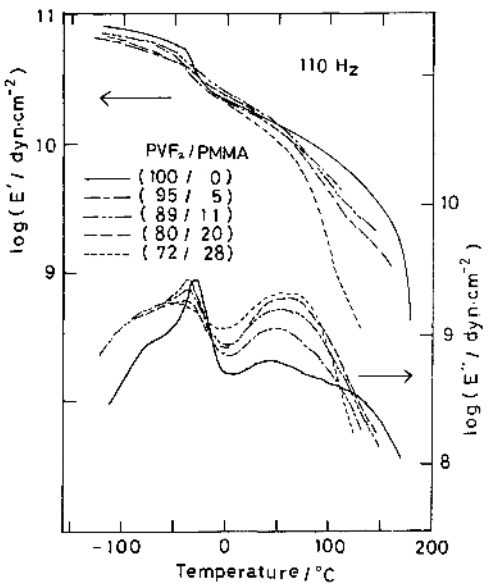

Figure 6. Temperature dependence of dynamic storage, E', and loss, E'', moduli at 110 Hz for semicrystalline MQ blends with $\phi_w > 0.70$.

blends with $0.7 \lesssim \phi_w \lesssim 0.82$, the two T_m's are plotted. For all these melt-mixed MQ and MA blends, we observe melting-point depressions roughly comparable to those in Nishi and Wang's results, which are shown in Figure 3 by a dashed curve. However, on examining these data more closely, we notice that the lower T_m's are nearly equal to those of the blends with $\phi_w \cong 0.6$, whereas the depression in the higher T_m's is somewhat less than that demonstrated by Nishi and Wang[3] for their solution-cast blends. This result might imply that a nearly pure PVF_2 phase still contains a small amount of PMMA, or this behavior might be a mere artifact due to a kinetic effect during the crystallization process.

Figure 4 shows the effect of the annealing temperature T_c on observed melting temperatures, T_m, for PVF_2 and several MA blends. In the range of T_c below 145°C, the T_m is nearly independent of T_c and is similar to that of the corresponding MQ blend. However, in the range of T_c above 145°C, the T_m's show a linear dependence on T_c. The T_m corresponding to the higher temperature peak extrapolates to the equilibrium melting point T_m° ($\simeq$188°C) of form II PVF_2 crystals,[11] whereas that of the lower temperature peak converges to a value ($\simeq$178°C) which is about 10°C lower than the T_m°. Nishi and Wang[3] also reported similar behavior in which the values extrapolated from the T_m's of their solvent-cast blends are somewhat lower than that of pure PVF_2, *e.g.*, 8.6°C for (50/50) blend and 4.0°C for (82.5/17.5) blend.[3] The PVF_2 crystals in their solvent-cast blends are presumably in equilibrium, or more precisely, in a quasiequilibrium state with the amorphous mixture, and hence are different from form II crystals. In our experiments the crystals with the lower peak temperature are presumably equivalent to the crystals of their solvent-cast blends and might possibly have resulted

from the amorphous mixture with $\phi_w \cong 0.6$, whereas those having the higher peak temperatures are grown from the nearly pure amorphous PVF_2 phase.

(b) Viscoelastic behavior. Figures 5 and 6 show plots of the dynamic storage modulus, E', and the dynamic loss modulus, E'', *versus* temperature (observed at a frequency of 110 Hz) for PMMA II and PVF_2/PMMA II MQ blends with $\phi_w \lesssim 0.5$ and for those with $\phi_w > 0.7$ and PVF_2, respectively. For the former series the temperature, at which a sharp decrease in log E' and a peak in log E'' occur, gradually shifts from the glass transition, T_g^{PMMA} ($\simeq 131$°C in this experiment), of PMMA to a lower temperature, as the PVF_2 content increases. This temperature apparently corresponds to the T_g of the amorphous mixture, which we denote as T_g^b. For the MQ 50/50 blend, small peaks appear in both the log E' and log E'' curves immediately after the main glass transition at T_g^b. These small peaks are evidently due to the crystallization and remelting of PVF_2 crystals from the amorphous blend, such as were seen in the DSC thermograms (*cf.* Figure 1). On the other hand, for the latter series the temperature, at which log E' sharply decreases and log E'' exhibits a peak, no longer changes with PVF_2 content but remains at about 45°C, which corresponds to the T_g^b of the MQ (60/40) blend. Furthermore, the height of (or the area under) the log E'' peak at about 45°C decreases, while a new peak appears at about −40°C and becomes sharper, as the PVF_2 content is increased above $\phi_w \cong 0.6$. The low temperature dispersion corresponds roughly to the $T_g^{PVF_2}$ of pure PVF_2. It should be noted that the area under the new peak appears to remain unchanged even with further increase in the PVF_2 content. This result implies that the increase in the PVF_2 content above $\phi_w \cong 0.6$ contributes mainly to the increase in the crystalline regions but not much to that in the amorphous phase (*cf.* Figure 2). In Figure 6 we also notice two other transitions at about −80°C and 150°C. Although the nature of such transitions is not clear at the moment, the former might be related to a secondary transition of the polymers, and the latter to the crystalline relaxation of PVF_2.

In Figure 7 these T_g values are plotted against the PVF_2 content, ϕ_w. The T_g^b data for the amorphous mixture with $\phi_w \lesssim 0.6$ closely fit the Gordon–Taylor equation proposed for compatible blends and

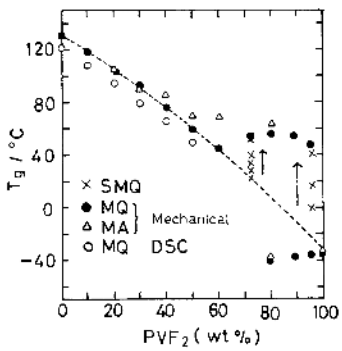

Figure 7. Dependence of glass-transition temperatures, T_g, on the PVF_2 content, ϕ_w, determined by DSC and dynamic mechanical experiments for melt-mixed and solution-mixed blends. Dashed curve represents the dependence predicted by the Gordon–Taylor equation. Arrows indicate the direction of increasing melt-annealing time, t, for SM (t min) Q blends. (*cf.* Figures 8 and 9).

copolymers:[12]

$$(T_g^{PMMA} - T_g^b)(1-\phi_w) + k(T_g^{PVF_2} - T_g^b)\phi_w = 0$$

where k is $\Delta\alpha_{PVF_2}/\Delta\alpha_{PMMA}$ and $\Delta\alpha$'s are the difference between the thermal expansion coefficients below and above the T_g's of the homopolymers. For example, plots of T_g^b *versus* $(T_g^{PMMA} - T_g^b)(1-\phi_w)/\phi_w$ give a straight line, which gives $k = 1.35$ from the slope and $T_g^{PVF_2} = -35$°C from the intercept. Similar plots of the DSC data (with $T_g^{PMMA} = 120$°C) gave $k = 1.35$ and $T_g^{PVF_2} = -50$°C. These values are in reasonably good agreement with literature values.[1,3,13,14] Using these values, we recalculated and plotted the T_g^b according to the Gordon–Taylor equation. The result is shown in Figure 7 by a dashed curve. The MQ blends with ϕ_w below 0.6 and the MA blends with ϕ_w below 0.5 possess only one T_g^b for each, and hence presumably a single amorphous blend phase, while the MA blends with ϕ_w above these critical values possess two glass transitions for each phase. The T_g at higher temperature corresponds to the T_g of the amorphous blend with the critical composition and the T_g at lower temperature to the T_g of pure PVF_2.

Behavior of Solution Mixed Blends

Figure 8 shows plots of log E' and log E'' *versus* temperature for an S blend and an SM (10 min) Q blend with 72/28 composition. The as-cast (S) blend

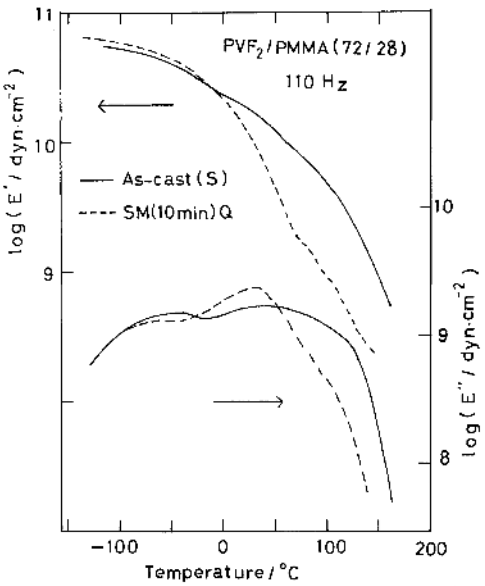

Figure 8. Temperature dependence of dynamic storage, E', and loss, E'', moduli at 110 Hz for a solvent-cast (S) and an SM (10 min) Q (72/28) blends.

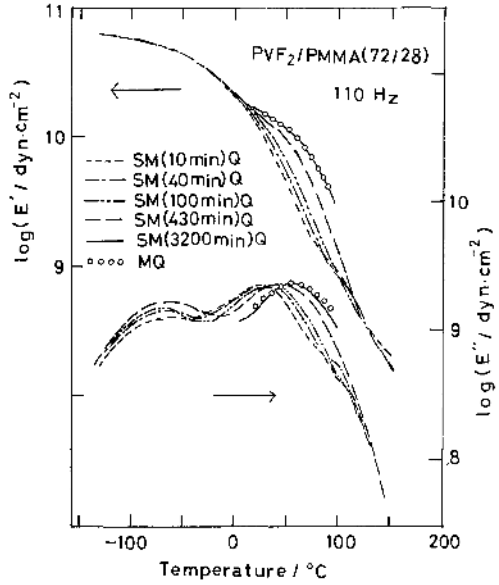

Figure 9. Variation with melt-annealing time, t, at 200°C of temperature dependence of dynamic storage, E', and loss, E'', moduli at 110 Hz for an SM (t min) Q (72:28) blend. Circles are the data for an MQ (72:28) blend covering the glass transition region.

temperature peaks. The thermograms were not normalized, and therefore are incapable of an absolute comparison.

exhibits a slow decrease in log E' and two broad peaks in log E''. A microscopic observation under polarized light on this blend revealed the presence of many small spherulites. The SM (10 min) Q blend exhibits at about 27°C a glass transition, which still differs significantly from the T_g^b ($\simeq$55°C) for the corresponding MQ (72/28) blend (*cf.* Figure 6). Figure 9 shows similar plots for the SM (t min) Q (72/28) blends with various melt-annealing time t. For comparison, the data for the MQ (72/28) blend in the T_g^b region are shown in the same figure. Apparently the temperature dispersion curve for the SM (t min) Q blends gradually shifts to that of the MQ blend. After 3200 minutes of melt-annealing, the two curves virtually coincide. Similar behavior was observed for a series of SM (t min) Q (95/5) blends. The SM (10 min) Q blend exhibited a sharp peak at the $T_g^{PVF_2}$ and a broad shoulder at about 20°C, which corresponds to a T_g^b of an amorphous blend with high PVF_2 content. For this system, too, the temperature dispersion curve gradually shifted to that of the MQ blend, as the melt-annealing time t increased. After 3400 minutes, the two curves nearly coincided with each other.

For comparison, in Figure 7 we plotted the values of T_g^b for the SM (t min) Q (72/28) and (95/5) blends. Apparently, by prolonged melt-annealing at 200°C of the SMQ blends, the T_g^b of the SMQ blends approach the T_g^b of the MQ blends. This behavior probably explains the reason for the discrepancy found between the T_g^b *versus* ϕ_w relations for melt-mixed blends of Paul *et al.*[2] and for solution-mixed blends of Nishi and Wang.[3]

The results in this and preceding sections suggest that the solution-mixed and melt-mixed blends with ϕ_w above 0.6 may take on different morphologies. In the former, the two components are more thoroughly mixed with each other. However, when the S blend is kept in the molten state at 200°C, phase separation takes place and the morphology gradually approaches the equilibrium state in which a mixture with $\phi_w \cong 0.6$ and a nearly pure PVF_2 melt are in the equilibrium. The LCST for this particular system might be about as low as or below 200°C.

Effects of Molecular Weights of PMMA

Table II demonstrates the effects of the molecular

Table II. Dependence of T_g and T_m on the molecular weight of PMMA in melt-quenched blends with PVF_2/PMMA (50/50) and (80/20) compositions

Sample	T_g/°C (from E″)	T_g/°C (from DSC)	Crystallinity in PVF_2 %	T_m/°C
(50/50 by weight)				
PVF_2/PMMA I	58	49	0	(160)[a]
PVF_2/PMMA II	60	50	0	(159)[a]
PVF_2/PMMA III	61	50	0	(158)[a]
(80/20 by weight)				
PVF_2/PMMA I	58 −40	Not detectable	62	172 161
PVF_2/PMMA II	56 −40	Not detectable	60	170 160
PVF_2/PMMA III	56	Not detectable	35	160

[a] PVF_2 crystals develop during the heating process (rate, 10°C min^{-1}) in DSC experiments.

weight of the PMMA component on the thermal and viscoelastic behavior of the blends. In the table, the T_g, T_m and the degree of crystallinity from DSC, and the T_g from dynamic mechanical experiments are compared for the MQ (50/50) and (80/20) blends in which the PVF_2 is mixed with three PMMA samples. For the three MQ (50/50) blends, virtually no molecular-weight effects are found. For the MQ (80/20) blends, however, those containing PMMA I and II exhibit two T_g's and two T_m's, while the one containing PMMA III exhibits only one T_g and one T_m. This imply that in the PVF_2/PMMA III (80/20) MQ blends, the two components are still mixed in the melt and the phase separation does not fully proceed.

DISCUSSION

The thermal and viscoelastic behavior of PVF_2/PMMA II melt-mixed blends may be summarized as follows. For the blends with $\phi_w < 0.4$, the two components are uniformly mixed in the melt (at 200°C). No crystallization may take place either by quenching from the melt or by subsequent annealing of the MQ blend at a temperature above its glass transition. Only one mixed amorphous phase exists in the blends. The glass-transition temperature obeys the Gordon–Taylor equation, and hence we denote it as T_g^b. For the blends with $0.4 < \phi_w < 0.5$, the two components are miscible in the melt as well as in the quenched solid exhibiting only one T_g^b. However, annealing of the quenched solid at a temperature above T_g^b results in the formation of PVF_2 crystals having one T_m that is subject to melting-point depression as described by Nishi and Wang.[3] We tentatively denote these crystals as "β-crystallites," meaning those crystals which have grown out of the "blends." The T_m of the "β-crystallites" drops considerably with a decrease in the PVF_2 content, suggesting that the "β-crystallites" are imperfect and contain an amorphous mixture entrapped between the crystalline lamellae.

For the blends with $\phi_w \cong 0.6$, the two components are barely mixed with each other in the melt and in the quenched solid. The ϕ_w is sufficiently large so that the crystallization of PVF_2 can proceed, yielding "β-crystallites," during the rapid reheating process in the DSC experiment. Possibly, phase separation on a microscopic scale might have taken place even in the melt. The PVF_2 microdomains might act as nuclei for rapid crystallization during the DSC experiment.

When ϕ_w is further increased to, say, 0.8, phase separation further proceeds in the melt, and a blend phase with $\phi_w \cong 0.6$ and a nearly pure PVF_2 melt might result. The quenching of such a melt yields a multiphase system consisting presumably of a mixed amorphous phase with $\phi_w \cong 0.6$, a "β-crystalline

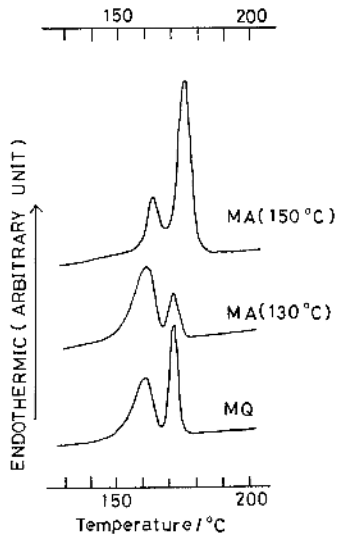

Figure 10. DSC thermograms for PVF_2 melting regions of PVF_2/PMMA II (80/20) MA (150°C), MA (130°C), and MQ blends, indicating the effect of the annealing temperature, T_c, on the low and high temperature peaks. The thermograms were not normalized, and therefore are incapable of an absolute comparison.

phase" grown out of the mixed phase, and a nearly pure semicrystalline PVF_2 phase. The semicrystalline phase is, more strictly speaking, composed of an amorphous PVF_2 phase and a form II PVF_2 crystalline phase. Thus the MQ (80/20) blend exhibits two T_g's and two T_m's. The T_g at the higher temperature is T_g^b for the mixture with $\phi_w \cong 0.6$ and that at the lower temperature is $T_g^{PVF_2}$. On the other hand, the T_m at the lower temperature is that for the "β-crystallites" and that at the high temperarure is for the form II PVF_2 crystallites. Annealing of the MQ (80/20) blend results in the development of the crystalline regions. However, the effect of the annealing temperature, T_c, is quite interesting, as demonstrated in Figure 10. Since the chromatograms are not normalized, a direct comparison of the absolute magnitudes of the components is not possible. However, the results clearly indicates that annealing at 130°C, being close to T_g^{PMMA}, reduces form II crystallites but develops "β-crystallites" considerably. On the other hand, an annealing at 150°C does the reverse.

We have attempted to elucidate the crystalline structures of these crystallites by a wide-angle X-ray diffraction method. However, so far no success has been achieved, because the degree of crystallinity relative to the whole blend specimen is too low and the structures themselves are too imperfect to yield clear diffraction data.

For melt-mixed MQ and MA blends with $\phi_w = 0.95$, nearly pure PVF_2 domains are predominantly large in comparison with mixed domains. Thus, we observe only one $T_g^{PVF_2}$ and only one T_m corresponding to form II crystallites, and the contributions from the blend phase are not clear.

For solution mixed as-cast (S) blends that have never been heated to a high temperature above the possible LCST around 200°C for a sufficiently long period of time, the two components are uniformly mixed and the blend exhibits only one T_g^b and one T_m (if $\phi_w > 0.5$). PVF_2 crystallites, which are presumably what we have denoted as "β-crystallites," develop during the DSC experiment or even by quenching provided $\phi_w > 0.7$.[3] For such blends the degree of crystallinity is usually quite low and the T_m drops considerably with an decrease in ϕ_w.[3] In this sense our present results on the multiphase behavior of the melt-mixed blends with high ϕ_w ($\gtrsim 0.7$) may not contradict previously reported results[1-3] of others, notably those of Nishi and Wang.[3] Whatever contradictions there may be are apparently due to differences in temperature and the period of heat treatment of the blends. The LCST of this system appears to be much lower than that suggested earlier by Paul *et al.*[6] This being the case, how has such a multiphase morphology came about? Previously, for compatible blends of melt-mixed amorphous polymer/semicrystalline polymer systems, Stein *et al.*[15,16] demonstrated from small-angle X-ray and light-scattering studies that in a certain system such as poly(ε-caprolactone)–poly(vinyl chloride) (PCL/PVC) blends, the amorphous component is entrapped in the interlamellar region as an amorphous phase, while in another system such as isotactic polystyrene–atactic polystyrene (*it*-PS/*at*-PS) blends, a segregation of the atactic component occurs during crystallization within the growing spherulite, forming interspherulitic mixed amorphous domains.

This kind of kinetic effect during crystallization might be responsible for the effect of the annealing temperature, T_c, on the behavior of the MQ (80/20) blend shown in Figure 10. That is, during annealing at 150°C, the PMMA component is segregated from

the interlamellar region to the interspherulitic region, while during the annealing at 130°C the PMMA component is hardly mobile but the amorphous PVF_2 component tends to mix with the entrapped PMMA component.

However, it is rather unlikely that this kind of the kinetic effect during crystallization is responsible for the multiphase behavior and the formation of the two different crystallites in the MQ (72/28) and (80/20) blends. As was evident from the behavior of SMQ blends, a few hours of melt-annealing were necessary for an SMQ blend to approach the behavior of an MQ blend. That is, the rate constant for this process is of the order of hours, and it is impossible for this process to be completed within a matter of seconds during the quenching process. A liquid-liquid phase separation must take place in the molten blend before a solid-liquid phase separation takes place during crystallization by quenching from the melt. In which case, another kind of kinetic process must be effective in such a liquid-liquid phase separation process. The 15 times repetition of the melting-quenching process is enough for the PVF_2/PMMA II MQ blends to reach an equilibrium or a quasiequilibrium state. However, the same procedure might not be sufficient for PVF_2/PMMA III (80/20) to reach equilibrium. This explains the peculiar dependence of the phase-separation behavior of the PVF_2/PMMA blends on the molecular weight of the PMMA component, such as shown in Table II. The PVF_2/PMMA III (80/20) blend must have a lower cloud point than either the PVF_2/PMMA I or PVF_2/PMMA II blends. Nevertheless, the former exhibited no evidence of a liquid-liquid phase separation but only one T_g[h] and one T_m for "β-crystallites." In other words, the former shows the typical two-phase behavior of a compatible semicrystalline polymer blend, in which only a solid-liquid phase separation takes place. On the other hand, the latter two blends show the four-phase behavior of an incompatible or a semicompatible, semicrystalline polymer blend, in which both a liquid-liquid phase separation in the melt and a solid-liquid phase separation may take place during the quenching process. Here we must make one more comment on the molecular-weight dependence of the pahse-separation behavior of this system. For the molecular-weight dependence, an effect of the PVF_2 domain size rather than the kinetic effect might be responsible. A melt, containing PMMA of a larger molecular weight, might have the mixed domains of a larger size and hence the PVF_2 domains of a smaller size which might yield only "β-crystallites" when quenched from the melt.

Acknowledgement. We wish to thank Mr. Shinsaku Uemura for his valuable advice on carrying out these experiments. This work was supported in part by the Ministry of Education, Science, and Culture under a Grant B 347081 to TK during 1976—1977.

REFERENCES

1. J. S. Noland, N. N.-C. Hsu, R. Saxon, and J. M. Schmitt, *Adv. Chem. Ser.*, **No. 99**, 15 (1971).
2. D. R. Paul and J. O. Altamirano, *Polym. Prepr., Am. Chem. Soc., Div. Polym. Chem.*, **15**, 409 (1974).
3. T. Nishi and T. T. Wang, *Macromolecules*, **8**, 909 (1975).
4. G. D. Patterson, T. Nishi, and T. T. Wang, *Macromolecules*, **9**, 603 (1976).
5. D. J. Hourston and I. D. Hughes, *Polymer*, **18**, 1175 (1977).
6. R. E. Bernstein, C. A. Cruz, D. R. Paul, and J. W. Barlow, *Macromolecules*, **10**, 681 (1977).
7. H. Lee, R. E. Salomon, and M. M. Labes, *Macromolecules*, **11**, 171 (1978).
8. D. C. Douglass and V. J. McBrierty, *Macromolecules*, **11**, 766 (1978).
9. T. Nishi, Kobunshi, **27**, 483 (1977); *J. Macromol. Sci., Phys.*, **B17** (1980) in press.
10. Y. Hirata, MS dissertation, Department of Macromolecular Science, Osaka University, 1979; Y. Hirata, S. Uemura, and T. Kotaka, *Rep. Prog. Polym. Phys., Jpn.*, **22**, 177 (1979).
11. K. Nakagawa and Y. Ishida, *J. Polym. Sci., Polym. Phys. Ed.*, **11**, 2153 (1973); S. Osaki and Y. Ishida, *J. Polym. Sci., Polym. Phys. Ed.*, **13**, 1071 (1975).
12. M. Gordon and J. S. Taylor, *J. Appl. Chem.*, **2**, 493 (1952).
13. G. M. Martin, S. S. Rogers, and L. Mandelkern, *J. Polym. Sci.*, **20**, 579 (1956).
14. L. Mandelkern, G. M. Martin, and F. A. Quinn, Jr., *J. Res. Natl. Bur. Stand.*, **58**, 137 (1957).
15. See, for exmple, F. B. Khambatta, F. Warner, T. Russell, and R. S. Stein, *J. Polym. Sci., Polym. Phys. Ed.*, **14**, 1391 (1976); R. S. Stein and T. Russell, Proceedings of The US-Japan Joint Seminar on Multicomponent Polymers, Kyoto, December 17–22, 1978; *J. Macromol. Sci., Phys.*, **B17** No. 2–4 (1980).